Measurements of Glucose Phosphorylation with FDG and PET Are Not Reduced by Dephosphorylation of FDG-6-phosphate

Hiroto Kuwabara and Albert Gjedde

Positron Imaging Laboratories, McConnell Brain Imaging Center, Montreal Neurological Institute, Montreal, Canada

To improve the measurements of glucose metabolism in the human brain, we imposed biologic constraints on the deoxyglucose model with and without dephosphorylation of FDG-6-phosphate (the k_4^*- and k_3^*-models). The constraints included constant transport and phosphorylation ratios (τ and φ) and a common partition volume (K_1/k_2) for tracer [^{18}F]FDG and glucose. In the presence of significant dephosphorylation, the k_3^*-model yielded time-dependent estimates of the phosphorylation coefficient (k_3^*), while the k_4^*-model yielded time-independent estimates. However, the two models yielded practically identical measurements of regional cerebral glucose metabolism in PET studies of six normal volunteers when the phosphorylation affinity ratio (the k_3^*/k_3 ratio of FDG and glucose) and tracer circulation time were 0.30 and 20 min for the k_3^*-model and 0.33 and 45 min for the k_4^*-model.

J Nucl Med 1991;32:692–698

To improve the measurements of regional cerebral glucose metabolism in humans, we imposed biologic constraints on the deoxyglucose model parameters in a previous paper (*1*). The constraints followed the original assumption of Sokoloff et al. (*2*) that both transport across the blood-brain barrier (BBB) and phosphorylation by hexokinase of tracer and native glucose obey Michaelis-Menten kinetics. Unlike the lumped constant, the transport and phosphorylation ratios between tracer and glucose are physiologic constants (τ and φ) (*3–5*). The brain glucose content can be determined from the partition volume of a hexose tracer (*6*). Thus, the transfer coefficients of glucose can be derived directly from the corresponding estimates of tracer, if the values of τ xand φ are known. The use of constraints enabled us to determine the regional cerebral glucose metabolism in 20 min after injection of tracer [^{18}F]fluorodeoxyglucose (FDG) (*1*).

We raised the question: Are measurements of regional cerebral glucose utilization affected by the dephosphorylation of FDG-6 phosphate? Phelps et al. and Huang et al. demonstrated that inclusion of a dephosphorylation coefficient (k_4^*) is appropriate for the human brain (*7,8*), and that the rate of radioactivity accumulation in brain (i.e., the net clearance K^*) reaches zero at 80–100 min after injection of tracer FDG. Therefore, when the k_4^* term is not included in the model, the K^* term, and consequently the phosphorylation coefficient (k_3^*) must decline as a function of time after introduction of tracer.

However, from a practical point of view, the advantage of the k_3^*-model, if equally appropriate, is that it yields more precise measurements of glucose utilization with one parameter less in a shorter time than does the k_4^*-model. For this reason, we investigated whether it was possible to eliminate the effect of dephosphorylation in the k_3^*-model by adjusting the phosphorylation ratio to the correct value. The constraints permit this adjustment because the apparent value of $\varphi(=k_3^*/k_3$-ratio, Equation 3) changes as a function both of the circulation time and the regional velocity of the dephosphorylation reaction. A global adjustment is possible if the use of the k_3^*-model is limited to short circulation times (i.e., 20 min) during which the effect of regional variations of the dephosphorylation is minimal.

First, we investigated whether φ values exist that cause the k_3 estimates for native glucose to agree for the two models. Second, we answered the question whether the two models yield identical estimates of the transport and utilization of glucose. In theory, the best estimate of k_4^* is one that eliminates the time-dependence of the K^* and k_3^* estimates observed with the k_3^*-model. Hence, third, we demonstrated that the constraints allowed us to find such values of k_4^*.

METHODS

To estimate the transfer coefficients of FDG, we extended the linear, multivariate, least-squares regression method of Blomqvist (*10*) to include the dephosphorylation coefficient of FDG-6-phosphate (k_4^*) and the correction for the cerebral vascular volume in the tissue (V_0) (*11–13*):

$$A^*(T) = \beta_1 C_a^*(T) + \beta_2 \int_0^T C_a^*(t)dt + \beta_3 \int_0^T \int_0^u C_a^*(t)dtdu + \beta_4 \int_0^T A^*(t)dt + \beta_5 \int_0^T \int_0^u A^*(t)dtdu, \quad \text{Eq. 1}$$

Received May 3, 1990; revision accepted Nov. 19, 1990.

For reprints contact Hiroto Kuwabara, MD, PhD, WB 213, Webster Pavillion, Montreal Neurological Institute, 3801 University, Montreal, Quebec H3A 2B4 Canada.

where $A^*(t)$ and $C_a^*(t)$ are radioactivities observed per cm^3 of brain tissue and per ml of arterial plasma, respectively, where

$$\begin{cases} \beta_1 = V_0 \\ \beta_2 = K_1^* + (k_2^* + k_3^* + k_4^*)V_0 \\ \beta_3 = K_1^*(k_3^* + k_4^*) + k_2^*k_4^*V_0 \\ \beta_4 = -(k_2^* + k_3^* + k_4^*) \\ \beta_5 = -k_2^*k_4^* \end{cases} \quad \text{Eq. 2}$$

and K_1^* is the unidirectional clearance from blood to brain, k_2^* the fractional clearance from brain to blood, and k_3^* the phosphorylation coefficient.

Constrained Method

The validity of the constraints was investigated in detail in a previous paper (*1*). In brief, the Michaelis-Menten kinetics assumes that the transport and phosphorylation ratios between FDG and glucose (τ and φ) are real constant (*3–5*) and that the partition volume (V_{k_1/k_2}) is common for tracer and native glucose and a function of brain glucose content (*6*). Mathematically, the constraints are given by:

$$\frac{K_1^*}{K_1} \cong \frac{K_t T_{max}^*}{K_t^* T_{max}} = \tau \text{ and } \frac{k_3^*}{k_3} = \frac{K_m V_{max}^*}{K_m^* V_{max}} = \varphi, \quad \text{Eq. 3}$$

where K_t and T_{max} are the Michaelis constant and maximal velocity of the transport and K_m and V_{max} the same for the phosphorylation reaction. Symbols with an asterisk (*) refer to FDG and those without refer to native glucose and,

$$V_c = \frac{K_1}{k_2} = \frac{K_1^*}{k_2^*} = \frac{K_t V_d + M_c}{K_t + C_a}, \quad \text{Eq. 4}$$

where M_c is glucose content in brain, C_a arterial plasma glucose concentration, and V_d the brain water volume.

The lumped constant (Λ) is the ratio between the net clearances of FDG and glucose in the k_3^*-model. In the k_4^*-model, we replaced the net clearance (zero in steady-state) with the unidirectional clearance from the circulation to the metabolic compartment ($K^* = K_1^*k_3^*/[k_2^* + k_3^*]$). This clearance reflects the fraction of FDG which is transported into the tissue from the circulation and further phosphorylated. The lumped constant is given by one equation, regardless of the model used:

$$\Lambda = \frac{K^*}{K} = \varphi + (\tau - \varphi)\frac{K^*}{K_1^*}. \quad \text{Eq. 5}$$

Note that the values of the K^* and Λ terms of the k_3^*-model decline with time when dephosphorylation occurs while those of the k_4^*-model may remain constant. In a previous paper (*1*), we redefined k_2^* and k_3^* in terms of K_1^* and K^*:

$$k_2^* = \frac{K_1^* + \mu K^*}{V_d} \text{ and } k_3^* = \frac{K^*}{K_1^* - K^*}\left[\frac{K_1^* + \mu K^*}{V_d}\right], \quad \text{Eq. 6}$$

where μ is $\tau C_a/[\Lambda K_t]$.

In the k_4^*-model, the coefficients K^*, K_1^*, k_4^*, and V_0 were estimated directly using Equations 1, 2, 5, and 6 using data obtained during the circulation of the tracer for 45 min. In the k_3^*-model, the same equations were used with k_4^* equal to zero and data obtained during the first 20 min of FDG circulation. The regional glucose phosphorylation rate (J_{net}) was calculated as:

$$J_{net} = \frac{K^*}{\Lambda} C_a, \quad \text{Eq. 7}$$

Conventional Method

In the conventional method, the coefficients K_1^*, k_2^*, k_3^*, k_4^*, and V_0 were estimated directly, using only Equations 1 and 2. The lumped constant was fixed at 0.48 in both the k_3^*- and k_4^*-models. In the k_3^*-model, k_4^* was zero. For both models, the tracer circulated for 45 min and J_{net} was calculated by Equation 7.

Choice of Constants of Constrained Method

In the presence of significant dephosphorylation of FDG-6-phosphate, the k_3^*-model requires an apparent value of φ which is different from the 'true' value in the k_4^*-model (see section 'Model-dependent φ values' in the discussion). Having previously chosen the most likely apparent value of φ for the k_3^*-model (0.30 at 20 min), we sought the value of φ for the k_4^*-model that minimized the difference between the regional k_3 values of glucose calculated from the k_3^* estimates ($k_3 = k_3^*/\varphi$) of the two models.

PET Studies

We reexamined previous PET studies (*1,12*). Briefly, dynamic measurements of J_{net} were made in six healthy, older volunteers (age 63 ± 3 yr) with the Therascan 3128 positron tomograph (*14*). The scan schedule was ten 1-min scans, five 2-min scans, and five 5-min scans, with a total of 20 scans in 45 min. Plasma radioactivity was determined as frequently as possible at first and then with progressively longer intervals, from the start of the slow (1 min) injection of FDG.

Fourteen gray matter structures, including the anterior and middle frontal, precentral, postcentral, posterioparietal, and occipital cortices, striatum, and thalamus were identified on the PET images on the basis of a standard anatomical atlas (*12*). The average size of the ROIs was 3.5 cm^2 (thickness 1.7 cm), and the arterial glucose levels of the subjects ranged from 4.8 to 6.8 m*M*.

Statistical Tests

The correlations between the regional estimates yielded by different methods, models, or conditions were expressed by the coefficient of linear correlation and/or the coefficient of root-mean-squared deviation (CORMSD), which is given by:

$$\text{CORMSD (\%)} = \sqrt{\frac{2}{n-1}\sum_{i=1}^{n}\left(\frac{E_{a_i} - E_{b_i}}{E_{a_i} + E_{b_i}}\right)^2} \times 100, \quad \text{Eq. 8}$$

where E_{a_i} and E_{b_i} are estimates of a variable in the ith region of interest (ROI) yielded by two fitting procedures to be compared and n the total number of ROIs examined ($n = 84$).

RESULTS

Choice of Constants for Constrained Method (k_4^*-model)

For different φ values of the k_4^*-model, we calculated regional phosphorylation coefficients of glucose (k_3) in the k_3^*- and k_4^*-models. The CORMSD between the k_3 estimates of the two models was smallest with φ values of 0.33, 0.34 and 0.35 (Fig. 1, upper panel). However, for values larger than 0.33, the k_3 estimates of the k_3^*-model exceeded those of the k_4^*-model in an increasing number

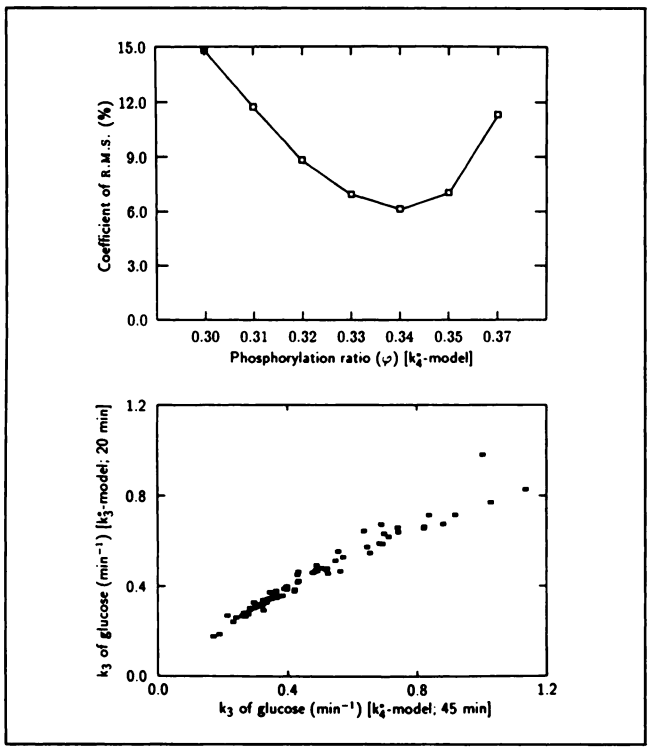

FIGURE 1. (Upper panel) CORMSD (%) between regional estimates of phosphorylation coefficient (k_3) of glucose, determined by k_3^*- and k_4^*-models, versus selected values of φ for k_4^*-model. Value of φ for k_3^*-model was fixed at 0.30, according to Kuwabara et al. (*1*). (Lower panel) Regional estimates of phosphorylation coefficient (k_3^*) of k_3^*-model vs. k_4^*-model for constrained method.

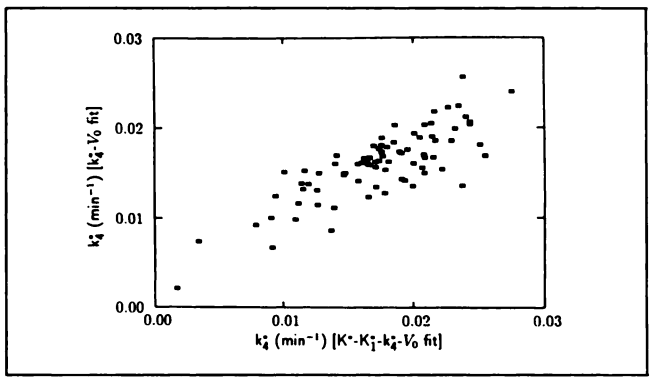

FIGURE 2. Regional estimates of k_4^* of k_4^*-V_0 fit versus estimates of k_4^* of K^*-K_1^*-k_4^*-V_0-fit (constrained method only, circulation time = 45 min). In k_4^*-V_0-fit, regional values of K_1^*, k_2^*, and k_3^* were fixed at the regional estimates of the k_3^*-model at 20 min and the k_3^* estimates were adjusted by the φ ratio (0.33/0.3). Regional estimates of k_4^* of two fits correlated well with each other.

of regions, as shown in the plot of the regional k_3 estimates of the two models (Fig. 1, lower panel). For this reason, we identified 0.33 as the "true" value of φ.

As shown in Equation 10, the 'true' magnitude of k_4^* in different regions may affect the estimates of k_3^* in the k_3^*-model. For this reason, we independently estimated k_4^* at 45 min using the K_1^*, k_2^*, and k_4^* estimates of the K_3^*-model obtained at 20 min as constants, the so-called k_4^*–V_0 fit, but adjusting the k_3^* estimates by the ratio between the true value of φ and the apparent value of φ obtained at 20 min in the k_3^*-model (0.33/0.30) to obtain the true and time-independent value of k_3^* in the k_4^*-model. The k_4^* estimates of the k_4^*–V_0 fit agreed well with those of the k_4^*-model at 45 min (the so-called K^*-K_1^*-k_4^*-V_0 fit) in most regions (Fig. 2). This indicates that the regional variations of dephosphorylation can be ignored at 20 min but become evident between 20 and 45 min.

Correlation Between Parameter Estimates of k_3^*- and k_4^*-models

The estimates of the transfer coefficients of FDG, the regionally calculated lumped constant (Λ), and the regional cerebral glucose utilization (J_{net}) determined by the k_3^*- and k_4^* models are listed in Table 1. On the basis of the constrained method, all variables of the two models were linearly correlated, although the estimates of k_3^*, K^* and Λ of the k_4^*-model exceeded the respective estimates of the k_3^*-model by CORMSD values of 17, 10, and 11%, respectively. With the conventional method, the correlation between the estimates of the same variables in the two models was poor except for the vascular volume (V_0).

Magnitude of k_4^* and Time-Constancy of the Remaining Estimates

The estimates of k_4^* averaged 0.018 ± 0.006 min^{-1} by the constrained method and 0.014 ± 0.009 min^{-1} by the conventional method. The k_3^*/k_4^* ratio was 8.6 by the constrained method and 6.9 by the conventional method.

For fixed values of k_4^*, the time-constancy of the remaining variables was evaluated between 20 min and 45 min (Table 2). The k_4^* value of 0.0068 min^{-1} (*6*) was associated with a 22% decline of the k_3^* estimates during this period. This value of k_4^* reduced, but did not eliminate, the time-dependency of K^* observed with the k_3^*-model (*1*). A larger value of k_4^* (0.0136 min^{-1}) further reduced the time-dependency of the estimates of k_3^*. When the regional estimates of k_4^* obtained at 45 min were used as fixed values in individual regions, estimates of all remaining variables were stable after 20 min, and the interregional relations were maintained perfectly.

Glucose Metabolism

Table 3 shows the mean ratios between the regional values of glucose utilization of the k_3^*- and k_4^*-models, according to the k_4^* values used in the analysis. When determined by the constrained method, the values of J_{net} of the two models were independent of the choice of value of k_4^* and practically identical (Fig. 3). The CORMSD between estimates of glucose utilization by the two models averaged 1.1% (range 0%–7%). When determined by the conventional method, the addition of k_4^* as a fixed value increased the estimates of J_{net} by 9% and 19% for the values of 0.0068 and 0.0136 min^{-1}, respectively. When

TABLE 1
Estimates of Transfer Coefficients of FDG and Their Correlations Between k_3^*- and k_4^*-models

Unit	Constrained Method: k_3^*-model	Constrained Method: k_4^*-model	Corr*	RM x CORMSD (%)†
K_1^* ml g^{-1} min^{-1}	0.087 ± 0.014	0.085 ± 0.014	0.96	2.8
k_2^* min^{-1}	0.203 ± 0.030	0.200 ± 0.030	0.98	1.9
k_3^* min^{-1}	0.127 ± 0.046	0.150 ± 0.064	0.94	15.0
k_4^* min^{-1}	—	0.018 ± 0.006	—	—
K^* ml g^{-1} min^{-1}	0.032 ± 0.006	0.035 ± 0.007	0.99	7.1
V_0 ml g^{-1}	0.033 ± 0.012	0.035 ± 0.012	0.92	7.2
V_e ml g^{-1}	0.43 ± 0.03	0.43 ± 0.03	0.98	1.3
Λ ratio	0.60 ± 0.06	0.65 ± 0.07	0.94	7.6
J_{net} μmol 100 g^{-1} min^{-1}	30.1 ± 5.4	29.2 ± 5.5	0.99	1.1
	Conventional Method			
	k_3^*-model	k_4^*-model	Corr*	RM x CORMSD (%)†
K_1^* ml g^{-1} min^{-1}	0.068 ± 0.011	0.077 ± 0.016	0.86	11.6
k_2^* min^{-1}	0.092 ± 0.039	0.146 ± 0.069	0.73	42.7
k_3^* min^{-1}	0.054 ± 0.012	0.098 ± 0.031	0.21	57.0
k_4^* min^{-1}	—	0.014 ± 0.009	—	—
K^* ml g^{-1} min^{-1}	0.026 ± 0.005	0.032 ± 0.005	0.61	20.2
V_0 ml g^{-1}	0.049 ± 0.017	0.044 ± 0.018	0.95	14.4
V_e ml g^{-1}	0.94 ± 0.60	0.74 ± 0.64	0.91	32.8
Λ ratio	(0.48)‡	(0.48)‡	—	—
J_{net} μmol 100 g^{-1} min^{-1}	30.5 ± 5.7‡	36.8 ± 6.5‡	0.63	20.2

* Coefficient of linear correlation.
† Coefficient of mean root-mean-squared deviation (%).
‡ In conventional method, a fixed lumped constant was used.

k_4^* was included as a parameter, the differences between the regional estimates of the two models were as large as 20% and the estimates were poorly correlated (r = 0.63, Table 1).

DISCUSSION

We have demonstrated that the use of biologic constraints interferes little with the appropriate description of the time course of tracer FDG and native glucose uptake into brain when the dephosphorylation coefficient k_4^* is included in the model (the k_4^*-model). We also demonstrated that a model without the k_4^* term (the k_3^*-model) yielded identical measurements of regional cerebral glucose utilization with only 20 min of tracer circulation.

The constrained method is a return to the original approach introduced by Sokoloff et al. (*2*); the movements of glucose and tracer are strictly related to each other at the two interfaces of the three-compartment model, i.e., at the BBB and at the enzyme hexokinase (*3–5*). Constant transport and phosphorylation ratios (τ and φ) replaced the lumped constant and described the uptake of tracer

TABLE 2
Effects of Fixed k_4^* Values on Time-Constancy of Remaining Estimates

	k_4^* = 0.0068 min^{-1}				k_4^* = 0.0136 min^{-1}				k_4^* = regional k_4^* (T = 45)			
	T = 20		T = 45	Corr*	T = 20		T = 45	Corr*	T = 20		T = 45	Corr*
K_1^*	0.086	↗	0.095	0.82	0.085	↗	0.090	0.86	0.084	→	0.085	0.98
k_2^*	0.199	↗	0.202	0.93	0.199	↗	0.207	0.94	0.196	→	0.197	0.99
k_3^*	0.134	↘	0.111	0.88	0.143	↘	0.129	0.90	0.151	→	0.149	0.97
K^*	0.033	↘	0.032	0.95	0.034	→	0.034	0.97	0.035	→	0.035	0.99
V_0	0.035	↘	0.024	0.45	0.035	↘	0.029	0.57	0.036	→	0.035	0.95
Λ	0.63	↘	0.59	0.69	0.64	↘	0.62	0.78	0.66	→	0.66	0.96
J_{net}	28.6	→	29.1	0.98	29.7	→	30.2	0.99	29.1	→	29.2	0.99

* Coefficient of linear correlation between T = 20 and T = 45 min.
Arrows indicate increase (↗), decreased (↘), or no change (→) at a 3% (mean RSD) level.

TABLE 3
k_4^* Values versus J_{net} Ratio of k_3^*-model and k_4^*-model

	J_{net} ratio : J_{net}[k_4^*-model]/J_{net}[k_3^*-model]		
k_4^* (min^{-1})	0.0068	0.0136	regional k_4^*
Constrained method	0.99 ± 0.03	1.00 ± 0.02	0.99 ± 0.01
Conventional method*	1.09 ± 0.02	1.19 ± 0.04	1.21 ± 0.13

Values are means and standard deviation.
* Mean values of J_{net} were different at 5% level, i.e., J_{net}[k_3^*-model] < J_{net}[$k_4^* = 0.0068$] < J_{net}[$k_4^* = 0.0136$] = J_{net}[$^*_4$-estimates].

into brain by two coefficients; the unidirectional rate of transport (K_1^*) and the unidirectional rate of phosphorylation (K^*). In a previous paper, we demonstrated that the use of the constraints corrected the uncertainty of the parameter estimates observed in the past; i.e., the partition volume (K_1/k_2) exceeding the physiologic limit (the brain water volume), and BBB transport (k_2^*) rather than hexokinase activity (k_3^*) regulating the uptake of FDG into brain (*1*).

Model-Dependent φ Values

When it is believed that the k_4^*-model is more appropriate for the human brain (*7,8*), the use of the k_3^*-model is valid only when the following conditions are met: (1) identical time courses of FDG and FDG-6-phosphate contents in brain ($M_e^*(t)$ and $M_m^*(t)$) predicted by the k_3^*- and k_4^*-models; and (2) identical transfer coefficients of native glucose predicted by the two models.

The content of FDG in brain at time t is given by:

$$M_e^*(t) = \frac{1}{k_2^*}\left[K_1^* C_a^*(t) - \frac{dM^*(t)}{dt}\right], \qquad \text{Eq. 9}$$

where $C_a^*(t)$ is arterial plasma radioactivity concentration of tracer and $M^*(t)$ total extravascular radioactivity content in brain at time t. When estimates of K_1^* and k_2^* of the two models are in good agreement, as in the case of the constrained method, condition 1 holds. In theory, transfer coefficients for the transport across the BBB (K_1^* and k^*) are model-independent because they are functions

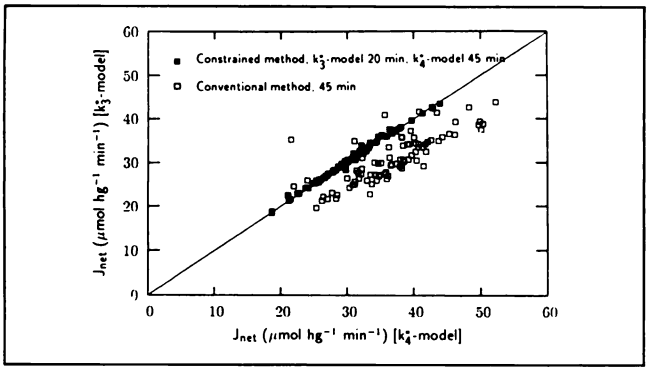

FIGURE 3. Estimates of cerebral glucose utilization (J_{net}) of k_3^*-model versus k_4^*-model for conventional (□) and constrained (■) methods of parameter estimation.

of the permeability-surface-area product and blood flow (*9*).

The k_3^* term, on the other hand, is specifically model-dependent. When condition 1 is met, the difference between the k_3^* estimates of the two models can be evaluated by the following equation:

$$\Delta k_3^* = k_{3(4)}^* - k_{3(3)}^* \cong k_4^* \frac{M_m^*(t)}{M_e^*(t)} > 0, \qquad \text{Eq. 10}$$

where the affixes 3 and 4 refer to the k_3^*- and k_4^*-models, respectively. Thus, when dephosphorylation does occur, the k_3^*-model underestimates the 'true' k_3^* estimates of the k_4^*-model. Model-dependent estimates of the k_3^*-model allowed us to use a time-dependent value of the phosphorylation affinity ratio (φ) in the k_3^*-model. Values of φ of 0.30 for the k_3^*-model and 0.33 for the k_4^*-model satisfied condition 2.

Equation 10 implies that regional variations of the phosphorylation reaction, if significant, may require regional adjustment of the φ value in the k_3^*-model. However, we found that regional variations were negligible for a global adjustment made at 20 min of tracer circulation for the k_3^*-model, although the regional variations became evident at 45 min (Fig. 2).

The original criteria for the derivation of values for the constants of the constraints (*1*) were a mean regional cortical glucose utilization in elderly controls of 30 μmol hg^{-1} min^{-1}, a partition volume of 0.43 ml g^{-1} (*15*), a lumped constant close to the value found in the literature (*16,17*), and transport and phosphorylation ratios (τ and φ) close to the respective values determined in animals (*3–5*).

Time Constancy of Estimates

The analytical model and the underlying physiology and biochemistry require that the transfer coefficients of the model are real constants. Thus, if the k_4^*-model is an appropriate description of the tracer uptake into brain, the estimates of transfer coefficients should remain constant with time after introduction of the tracer.

Several authors have argued that heterogeneous metabolism within a ROI, not unlikely in the relative large ROIs observed by PET, violates a precept of the original 2DG method and causes the observed k_3^* to decline as a function of time. Nelson et al. (*18*) explained the time-dependence on the grounds that tissue components with high values of k_3^* have high values of M_e^*(t) and that the value of $\overline{k_3^*}$ (see below) declines as regional differences of M_e^*(t) decrease with time.

When a ROI consists of n tissue units, in each of which we assume homogenous metabolism with K_1^*, k_2^*, and k_3^* values of $K_{1_i}^*$, $k_{2_i}^*$, and $k_{3_i}^*$, and a mass of w_i, the observed k_3^* value ($\overline{k_3^*}$) of the ROI is:

$$\overline{k_3^*} = \frac{\sum w_i k_{3_i}^* \int_0^T M_{e_i}^*(t)dt}{\sum w_i \int_0^T M_{e_i}^*(t)dt}. \qquad \text{Eq. 11}$$

Using $\int_0^T M_{c_i}^*(t)dt = V_{c_i}[\int_0^T C_a^*(t) - M_i^*(t)/K_{1_i}]$, the equation changes to,

$$\overline{k_3^*} = \frac{\sum_{i=1}^n w_i K_{i}^*(1 - Op_i)}{\sum_{i=1}^n w_i V_{c_i}(1 - Op_i)} \approx \frac{\sum w_i K_{i}^*}{\sum w_i V_{c_i}}, \quad \text{Eq. 12}$$

where $\rho_i = M_i^*(t)/[K_{1_i} \int_0^T C_a^*(t)]$ and K_{i}^* the total clearance $K_{1_i}^* k_{3_i}^*/k_{2_i}$. Variations of the ρ_i term can be expected to be extremely small, at least after 20 min, because $M_i^*(t) \ll \int_0^T C_a^*(t)$ and K_{1_i} is roughly proportional to $M_i^*(t)$. Thus, tissue heterogeneity alone is unlikely to cause a time-dependent decline of $\overline{k_3^*}$ estimates after 20 min from the introduction of the tracer.

We found that the regional k_4^* estimates at 45 min were the only k_4^* values that yielded time-constant estimates of other coefficients when used as fixed values in the fitting regression (Table 2). In contrast, when the k_4^* term was fixed to an arbitrary value of 0.0068 or 0.0136 min^{-1}, we found systematic deviation of other estimates between 20 and 45 min.

Significance of k_4^*

In a steady-state, the flux of metabolites by dephosphorylation (J_{out}^*) and further transport out of brain is:

$$J_{out}^* = k_4^* M_m^*(\infty) \cdot \left[\frac{k_2^*}{k_2^* + k_3^*}\right] = \frac{K_1^* k_3^*}{k_2^* + k_3^*} C_a^*(\infty), \quad \text{Eq. 13}$$

where $M_m^*(\infty)$ is $[K_1^* k_3^*]C_a^*(\infty)/[k_2^* k_4^*]$ in steady-state. Note that J_{out}^* is independent of k_4^*. Of course, the flux J_{out}^* should be the same as the flux J_{in}^* of tracer FDG transported from the circulation into brain and further phosphorylated,

$$J_{in}^* = K_1^* C_a^*(\infty) \cdot \left[\frac{k_3^*}{k_2^* + k_3^*}\right] = \frac{K_1^* k_3^*}{k_2^* + k_3^*} C_a^*(\infty). \quad \text{Eq. 14}$$

In fact, the significance of the k_4^* term is not to determine the loss of metabolites but to determine, together with the k_3^* term, the magnitude of the M_m^*/M_e^* ratio in steady-state. The high k_3^* and k_4^* values of the constrained method simply indicate that the exchange between the precursor and metabolic compartments was more vigorous than determined in previous longer studies (i.e., 3~5 hr) in which k_4^* averaged 0.055 – 0.075 min^{-1} (*7,11,19*). However, the k_3^*/k_4^* ratio was well within the range observed in the longer studies (8.5–12.5), especially when the brain vascular volume was taken into account (*11*).

The high k_3^* and k_4^* values of the constrained method were comparable to values estimated in biochemical studies. Some authors directly measured the contents of glucose analogues and their phosphated metabolites ($M_e^*(t)$ and $M_m^*(t)$) in brain biochemically or with magnetic resonance spectroscopy (*20–22*). When data of 45 min after introduction of tracer was fitted by the equation $M_m^*(t) = k_3^* \int_0^T M_e^*(t)dt - k_4^* \int_0^T M_m^*(t)dt$, the k_3^* estimates averaged 0.120–0.124 min^{-1} and k_4^* 0.015 – 0.023 min^{-1}.

The coefficient of variation of 84 regional k estimates for six healthy volunteers was 31% at 45 min with the constrained method, comparable to previous studies of longer duration (21%–41%) (*7,11,19*). Without constraints, the coefficients at 45 min were in the 60% range (Table 1) and (*17*).

Lumped Constant

The constrained method does not require explicit knowledge of Λ because the regional cerebral glucose utilization is, in fact, calculated by:

$$J_{net} = \frac{C_a}{\varphi/K^* + (\tau - \varphi)/K_1^*}, \quad \text{Eq. 15}$$

where C_a is the arterial plasma glucose concentration. The equation shows that the glucose utilization is given by two regional estimates and two constants assumed to have little regional or intersubject variation. With the constrained method, the two models yielded identical values for the regional cortical glucose utilization with the use of a time-dependent φ value in the k_3-model.

Reivich et al. (*16*) applied the original method of Sokoloff et al. (*2*) to human brain and experimentally measured the whole brain value of Λ as 0.52. To derive the value, the authors assumed no dephosphorylation of FDG-6-phosphate. However, on the basis of the k_4^*-model and with knowledge of the transfer coefficients, the authors suggested that the value of Λ could be determined by measuring arterio-venous differences of tracer and glucose. Using a method established for this purpose by Matsuda et al. (*23*), Redies and Diksic (*24*) obtained a value for FDG of 0.68 in ferrets in good agreement with the result of the present study.

ACKNOWLEDGMENTS

The authors thank the technicians of the Positron Imaging Laboratories, including the Medical Cyclotron and Radiochemistry facility, for their untiring and expert acquisition of the original positron tomographs of elderly volunteer subjects. The present study was supported by grants from the Quebec Heart Foundation and the Medical Research Council of Canada (PG-41).

REFERENCES

1. Kuwabara H, Evans AC, Gjedde A. Michaelis-Menten constraints improved cerebral glucose metabolism and regional lumped constant measurements with [^{18}F]fluorodeoxyglucose. *J Cereb Blood Flow Metab* 1990;10:180–189.
2. Sokoloff L, Reivich M, Kennedy C, et al. The [^{14}C]deoxyglucose method for the measurement of local cerebral glucose utilization: theory, procedure, and normal values in the conscious and anesthetized albino rat. *J Neurochem* 1977;28:897–916.
3. Cunningham VJ, Cremer JE. A method for the simultaneous estimation of regional rates of glucose influx and phosphorylation in rat brain using radiolabeled 2-deoxyglucose. *Brain Res* 1981;221:319–330.
4. Gjedde A. High- and low-affinity transport of D-glucose from blood to brain. *J Neurochem* 1981;36:1463–1471.
5. Crane PD, Pardridge WM, Braun LD, Oldendorf WH. Kinetics of transport and phosphorylation of 2-fluoro-2-deoxy-D-glucose in rat brain. *J Neurochem* 1983;40:160–167.
6. Gjedde A, Diemer NH. Autoradiographic determination of regional brain

glucose content. *J Cereb Blood Flow Metab* 1983;3:303–310.
7. Phelps ME, Huang SC, Hoffman EJ, Selin C, Sokoloff L, Kuhl DE. Tomographic measurement of local cerebral glucose metabolic rate in humans with (F-18)2-fluoro-2-deoxy-D-glucose: validation of method. *Ann Neurol* 1979;6:371–388.
8. Huang SC, Phelps ME, Hoffman EJ, Sideris K, Selin CJ, Kuhl DE. Noninvasive determination of local cerebral glucose metabolic rate of glucose in man. *Am J Physiol* 1980;238:E69–E82.
9. Gjedde A. Calculation of cerebral glucose phosphorylation from brain uptake of glucose analogs in vivo: a re-examination. *Brain Res Rev* 1982;4:237–274.
10. Blomqvist G. On the construction of functional maps in positron emission tomography. *J Cereb Blood Flow Metab* 1984;4:629–632.
11. Hawkins RA, Phelps ME, Huang SC. Effects of temporal sampling, glucose metabolic rates, and disruptions of the blood-brain barrier on the FDG model with and without a vascular compartment: studies in human brain tumor with PET. *J Cereb Blood Flow Metab* 1986;6:170–183.
12. Evans AC, Diksic M, Yamamoto YL, et al. Effect of vascular activity in the determination of rate constants for the uptake of ^{18}F-labeled 2-fluoro-2-deoxy-D-glucose: error analysis and normal values in older subjects. *J Cereb Blood Flow Metab* 1986;6:724–738.
13. Evans AC. A double integral form of the three compartmental, four rate-constant model for faster generation of parameter maps. *J Cereb Blood Flow Metab* 1987; 7(suppl 1):S453.
14. Cooke BE, Evans AC, Fanthome EO, Alaire R, Sendyk AM. Performance figures and images from the Therascan 3128 positron emission tomograph. *IEEE Trans Nucl Sci* 1984; NS-31(1):640–644.
15. Gjedde A, Wienhard K, Heiss W-D, et al. Comparative regional analysis of 2-fluorodeoxyglucose and methylglucose uptake in brain of four stroke patients with special reference to the regional estimation of the lumped constant. *J Cereb Blood Flow Metab* 1985;5:163–178.
16. Reivich M, Alavi A, Wolf A, et al. Glucose metabolic rate kinetic model parameter determination in humans: the lumped constants and rate constants for [^{18}F]fluorodeoxyglucose and [^{11}C]deoxyglucose. *J Cereb Blood Flow Metab* 1985;5:179–192.
17. Lammertsma AA, Brooks DJ, Frackowiak SJ, et al. Measurement of glucose utilization with [^{18}F]2-fluoro-2-deoxy-D-glucose: a comparison of different analytical methods. *J Cereb Blood Flow Metab* 1987;7:161–172.
18. Nelson T, Dienel GA, Mori K, Cruz NF, Sokoloff L. Deoxyglucose-6-phosphate stability in vivo and the deoxyglucose method: response to comments of Hawkins and Miller. *J Neurochem* 1987;49:1949–1960.
19. Reivich M, Kuhl D, Wolf A, et al. The [^{18}F]fluorodeoxyglucose method for the measurement of local cerebral glucose utilization in man. *Circ Res* 1979;44:127–137.
20. Deuel RK, Yue GM, Sherman DJ, Ackerman JJH. Monitoring the time course of cerebral deoxyglucose metabolism by ^{31}P nuclear magnetic resonance spectroscopy. *Science* 1985;288:1329–1330.
21. Nelson T, Lucignani G, Goochee J, Crane AM, Sokoloff L. Invalidity of criticisms of the deoxyglucose method based on alleged glucose-6-phosphatase activity in brain. *J Neurochem* 1986;46:905–919.
22. Pelligrino DA, Miletich DJ, Albrecht RF. Time course of radiolabeled 2-deoxy-D-glucose-6-phosphate turnover in cerebral cortex of goats. *Am J Physiol* 1987;252:R276–283.
23. Matsuda H, Nakai H, Jovkar S, et al. Alternative approach to estimate lumped constant in the deoxyglucose model: simulation and validation. *J Nucl Med* 1987;28:471–480.
24. Redies C, Diksic M. The deoxyglucose method in the ferret brain. I. Methodological consideration. *J Cereb Blood Flow Metab* 1989;9:35–42.

Erratum

In the "Nuclear Medicine Week Update" box (*Newsline. J Nucl Med* 1991;32:31N), the dates for NMW were printed incorrectly. The correct dates for NMW are ***July 28 through August 3.*** Articles in the May 1991 *Newsline* and June 1991 *JNMT* will preview this year's poster and button.